# Simple Application of Fictitious Crack Model in Reinforced Concrete Beams

Ulfkjær, J. P.; Hededal, O.; Kroon, I. B.; Brincker, Rune

*Publication date:*
1993

*Document Version*
Early version, also known as pre-print

Link to publication from Aalborg University

*Citation for published version (APA):*
Ulfkjær, J. P., Hededal, O., Kroon, I. B., & Brincker, R. (1993). *Simple Application of Fictitious Crack Model in Reinforced Concrete Beams*. Dept. of Building Technology and Structural Engineering, Aalborg University. Fracture and Dynamics Vol. R9349 No. 51

# INSTITUTTET FOR BYGNINGSTEKNIK
DEPT. OF BUILDING TECHNOLOGY AND STRUCTURAL ENGINEERING
AALBORG UNIVERSITETSCENTER • AUC • AALBORG • DANMARK



**FRACTURE & DYNAMICS**
**PAPER NO. 51**

**Presented at the IUTAM Symposium on Fracture of Brittle Disordered Materials: Concrete, Rock and Ceramics, University of Queensland, Australia, September 20-24, 1993**



**J. P. ULFKJÆR, O. HEDEDAL, I. B. KROON & R. BRINCKER**


**SIMPLE APPLICATION OF FICTITIOUS CRACK MODEL IN REINFORCED CONCRETE BEAMS**


**DECEMBER 1993** **ISSN 0902-7513 R9349**

INSTITUTTET FOR BYGNINGSTEKNIK
DEPT. OF BUILDING TECHNOLOGY AND STRUCTURAL ENGINEERING
AALBORG UNIVERSITETSCENTER • AUC • AALBORG • DANMARK

FRACTURE & DYNAMICS
PAPER NO. 51

Presented at the IUTAM Symposium on Fracture of Brittle Disordered Materials: Concrete, Rock and Ceramics, University of Queensland, Australia, September 20-24, 1993

J. P. ULFKJÆR, O. HEDEDAL, I. B. KROON & R. BRINCKER
SIMPLE APPLICATION OF FICTITIOUS CRACK MODEL IN REINFORCED CONCRETE BEAMS
DECEMBER 1993 ISSN 0902-7513 R9349

# SIMPLE APPLICATION OF FICTITIOUS CRACK MODEL IN REINFORCED CONCRETE BEAMS-ANALYSIS AND EXPERIMENTS

J.P. ULFKJÆR, O. HEDEDAL, I. KROON & R. BRINCKER
University of Aalborg, Aalborg, Denmark

Abstract
A previously presented method for fictitious crack propagation in plain concrete beams is extended to lightly reinforced concrete beams. The method is based on a continuous layer of springs in the midsection representing, the fictitious crack model and equilibrium conditions. The derivations are divided into three phases (linear elastic, development of fictitious crack and real crack growth) and each phase is divided into two situations (elastic or plastic behavior of the steel reinforcement). Even though the model is simple, it is able to capture some distinctive effects, i.e., the change in behavior from brittle to ductile when the reinforcement area is increased, and from ductile to brittle when the size scale is increased. Experiments are performed and comparisons show that the assumption of a linear softening relation is not adequate. It is also seen that the debonding problem needs to be taken into account.
Keywords: Fictitious Crack Model, Lightly Reinforced, Three Point Bending, Size Effects, Experiments.

## 1 Introduction

A variety of numerical methods based on the fictitious crack model exists which can be used to predict the load carrying capacity of plain and reinforced concrete structures, Modéer (1979), Van Mier (1989).

To the authors knowledge only one analytical model which describe crack propagation in reinforced concrete based on fracture mechanics exists, Bosco and Carpinteri (1990). The model is based on linear elastic fracture mechanics and assumes that the reinforcement behaves rigid-perfectly plastic. Their model is therefore especially applicable for brittle concrete beams.

In this paper we present a method based on the simplest possible version of the FC-model for a crack in a beam in bending.

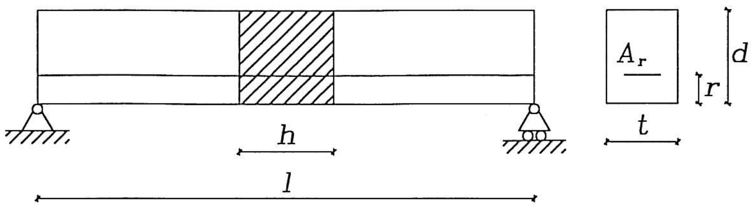


Fig. 1. The considered beam.

## 2 Basic Assumptions

The model is based on the approximations: 1) the response of the beam is represented by a thin layer of springs with thickness $h$ due to the crack, and 2) the softening relation is linear.

Consider the beam in Fig. 1 subjected to a rotational controlled load $\varphi$ ( the angle between the deflected beam and vertical ) with the reinforcement area $A_r$ in the depth $r$. The reinforcement is assumed to be linear elastic-perfectly plastic described by the modulus of elasticity, $E_s$ and the yield stress, $\sigma_y$. The concrete is described by the modulus of elasticity and the brittleness number, $B$. The brittleness number is a parameter including both the material parameters and the beam size $l$. In the present case the brittleness number $B$ is defined as

$$B = \frac{\sigma_u}{w_c}\frac{h}{E} = \frac{\sigma_u^2 h}{2G_F E} \tag{1}$$

where $E$ is the modulus of elasticity and the other parameters are defined in Fig. 2b. The thickness $h$ of the elastic layer is assumed to be proportional to the beam depth $h = kd$.

The assumption is validated by comparison of plain concrete beams with detailed numerical computations where $k$ is varied in order to obtain identical peak loads and thereby indicating a typical value of $k \simeq 0.5$, Ulfkjær et al. (1993).

The calculations are divided into three phases. Phase I): before the tensile strength is reached in the tensile side of the beam, phase II): development of a fictitious crack in the layer, and phase III): crack propagation. The phases and the corresponding stress distributions are indicated in Fig 2a. The state of the elastic layer is described by a uniform axial strain which in all phases vary linearly over the depth. Each phase is divided into two situations: a) the steel remains elastic or b) the steel yields. The strain condition in the steel in the elastic layer is assumed to follow the concrete strain of the layer.

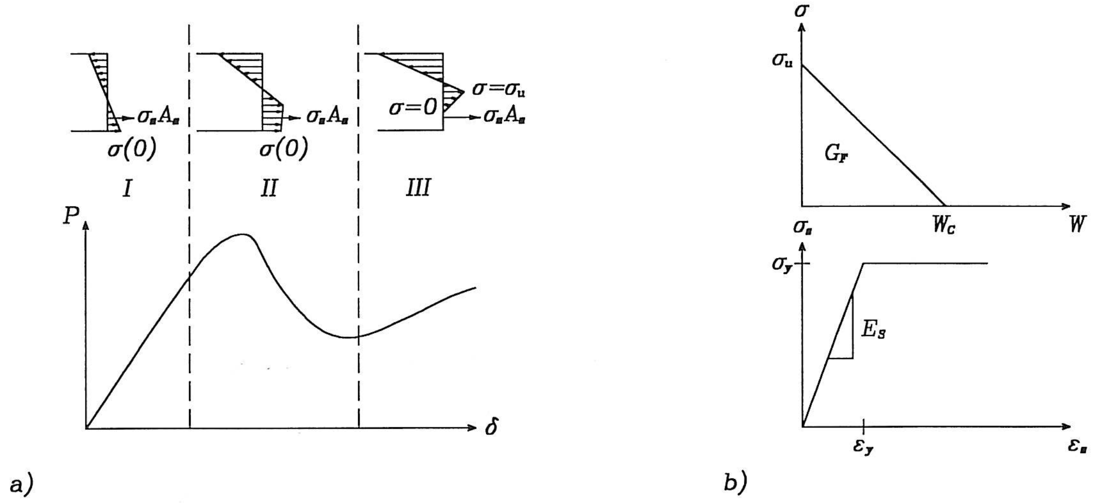


Fig. 2. a) Sketch of the load-displacement curve for reinforced concrete beams where the three phases are indicated. b) the constitutive relations for the concrete and the steel.

### 3 Solutions for Load-Displacement Curve

In the following the geometrical quantities are made non-dimensional by division with the beam depth.

Phase I.

In this phase the concrete is linear elastic. Horizontal equilibrium gives the normalized position of the neutral axis (measured from the bottom of the beam) $\alpha_\eta$

$$\alpha_\eta = \frac{1}{2}\left[\frac{1 + 2\zeta\rho\alpha_r}{1 + \zeta\rho}\right] \quad \text{for } \varepsilon_s \le \varepsilon_y \quad \vee \quad \alpha_\eta = \frac{1}{2}\left[1 - \rho\frac{\sigma_y}{\sigma_u}\frac{1}{\theta}\right] \quad \text{for } \varepsilon_s > \varepsilon_y \tag{2}$$

where, $\zeta = E_s/E$, is the flexibility ratio between steel and concrete, $\rho = A_r/td$, is the reinforcement ratio, $\alpha_r = r/d$, is the normalized position of the reinforcement, $\theta = \varphi E/k\sigma_u$ is a normalized rotation and $\epsilon_s$ is the steel strain. The equivalent moment, $\mu = 6M/td^2\sigma_u$ where $M$ is the bending moment becomes

$$\mu(\theta) = \theta(4 - 6\alpha_\eta) - 6\frac{\sigma_s(\theta)}{\sigma_u}\rho\alpha_r \tag{3}$$

where, $\sigma_s$ is the steel stresses. Thus, the moment rotation curve is linear in phase I if the steel is not yielding, and bi-linear if the steel yields. Phase I ends when the strain in the bottom equals, $\varepsilon_u$, yielding the following condition to the normalized rotation

$$\theta \le \frac{1}{2\alpha_\eta} \quad (4)$$

Phase II.

In phase II the fictitious crack develops. The size of the elastic tensile zone is found by the condition that the strain at the fictitious crack tip is $\varepsilon_u = \sigma_u / E$ giving $\alpha_\eta = 1/2\theta$. The position of the neutral axis is determined by taking horizontal equilibrium giving the size of the fictitious crack $\alpha_f$

$$\alpha_f = (1 + \zeta\rho)(1 - B) \pm \sqrt{(1 + \zeta\rho)^2(1 - B)^2 - (1 + 2\zeta\rho\alpha_r)(1 - B) + \frac{1}{\theta}(1 - B)(1 + \zeta\rho)} \quad \text{for } \varepsilon_s \le \varepsilon_y$$

$$\alpha_f = (1 - B) \pm \sqrt{\frac{1}{\theta}(1 - B)\left[1 + \frac{\sigma_y}{\sigma_u}\rho\right]} \qquad \text{for} \qquad \varepsilon_s > \varepsilon_y \quad (5)$$

and the equivalent moment becomes

$$\mu(\theta) = \theta\left[\frac{2\alpha_f(\theta)^3}{1 - B} - 6\alpha_f(\theta) + 4\right] - 3 + 6\frac{\sigma_s(\theta)}{\sigma_u}\rho\alpha_r \quad (6)$$

which is completely equivalent to the plain concrete model, Ulfkjær et al. (1993), except for the last term taking the steel into account.

Phase III.

In phase III the real crack starts to grow. The size of the elastic tensile zone is as in phase II, $\alpha_\eta = 1/2\theta$. By considering similar triangles the non-dimensional size $\alpha_f$ of the fictitious crack is determined as

$$\alpha_f = \left[\frac{1 - B}{B}\right]\frac{1}{2\theta} \quad (7)$$

Again this is equivalent to the plain concrete beam. The normalized length of the real crack, $\alpha$, is determined be requiring horizontal equilibrium

$$\alpha = 1 + \zeta\rho - \frac{1}{2B\theta} \pm \sqrt{\zeta\rho(\zeta\rho + 2(1 - \alpha_r)) + B\left(\frac{1}{2B\theta}\right)^2} \quad \text{for} \quad \varepsilon_s \leq \varepsilon_y$$

$$\alpha = 1 - \frac{1}{2B\theta} \pm \sqrt{2\rho\frac{\sigma_y}{\sigma_u}\frac{1}{2\theta} + B\left(\frac{1}{2B\theta}\right)^2} \quad \text{for} \quad \varepsilon_s > \varepsilon_y \qquad (8)$$

and the equivalent moment becomes

$$\mu(\theta) = \theta\left\{4 - 6\left(\frac{1}{2B\theta} + \alpha\right) + \frac{2(\alpha + \alpha_f)^2 - 2B\alpha^3}{1 - B}\right\} + 6\frac{\sigma_s}{\sigma_u}\rho\alpha_r \qquad (9)$$

Elastic deformations in the beam parts outside the elastic layer are taken into account by subtracting the elastic deformation $\mu(\theta)$ from the elastic layer leaving only deformations due to crack growth and then adding the elastic deformations of the whole beam using a solution for an elastic beam with a concentrated force given by, Timoshenko (1955). The central elastic beam deflection is

$$\delta_e = \frac{Ml^2}{12EI}\beta(\lambda) \qquad (10)$$

where $EI$ is the bending stiffness of the beam, and $\beta$ is a factor describing the influence of the concentrated load $\beta = 1 + 2.85/\lambda^2 - 0.84/\lambda^3$, and $\lambda$ is the slenderness ratio $\lambda = l/b$. Introducing the elastic rotation similar to equation (6)

$$\theta_e = 2\frac{\delta_e}{l}\frac{bE}{h\sigma_u} \qquad (11)$$

The relation (17) can be written in non-dimensional form

$$\theta_e = \gamma\mu \qquad (12)$$

where

$$\gamma = \frac{\beta}{3k\lambda} \qquad (13)$$

The effect of the beam flexibility is introduced by adding $\theta_e$ and subtracting the deformation of the elastic springs. Thus, the total deformation $\theta_t$ is

$$\theta_t = \theta + \theta_e - \mu = \theta + (\gamma - 1)\mu \qquad (14)$$

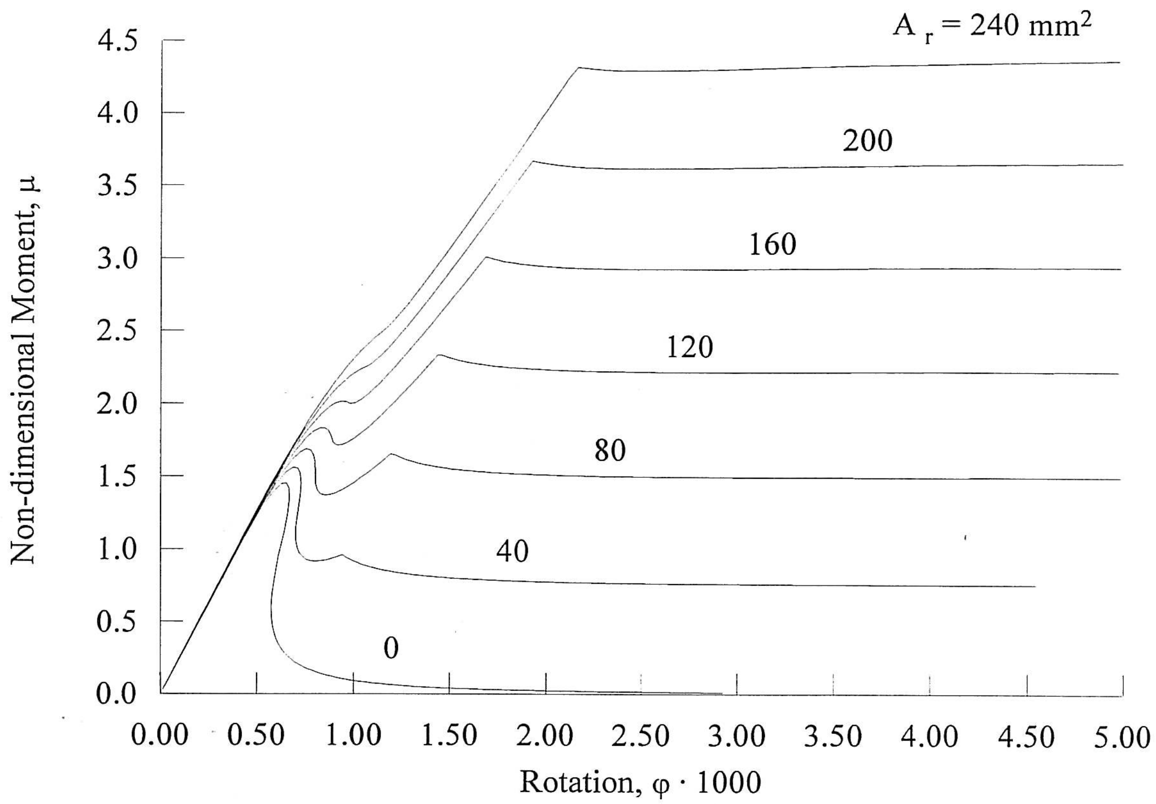


Fig. 3. Moment - rotation curves for beams with different reinforcement areas.

Table 1. Geometry and materials parameters for the beam at size scale 1

| | |
|---|---|
| Beam Depth, $d$ [mm] | 200.0 |
| Beam Width, $t$ [mm] | 200.0 |
| Beam Length, $l$ [mm] | 1600.0 |
| Specific Fracture Energy, $G_F$ [Nmm/mm$^2$] | 0.100 |
| Modulus of Elasticity, $E$ [N/mm$^2$] | 20,000 |
| Brittleness Number, $B$ [-] | 0.1125 |

## 4 Load-Displacement Curves

In Fig. 3 normalized moment-rotation curves as calculated using the method for the beam with the geometrical and constitutive parameters shown in table 1. (which corresponds to a medium sized beam of normal strength concrete) with different reinforcement areas are shown. In Fig. 4 normalized moment-rotation curves for the standard RILEM beam at different size scales with constant reinforcement ratios are shown.

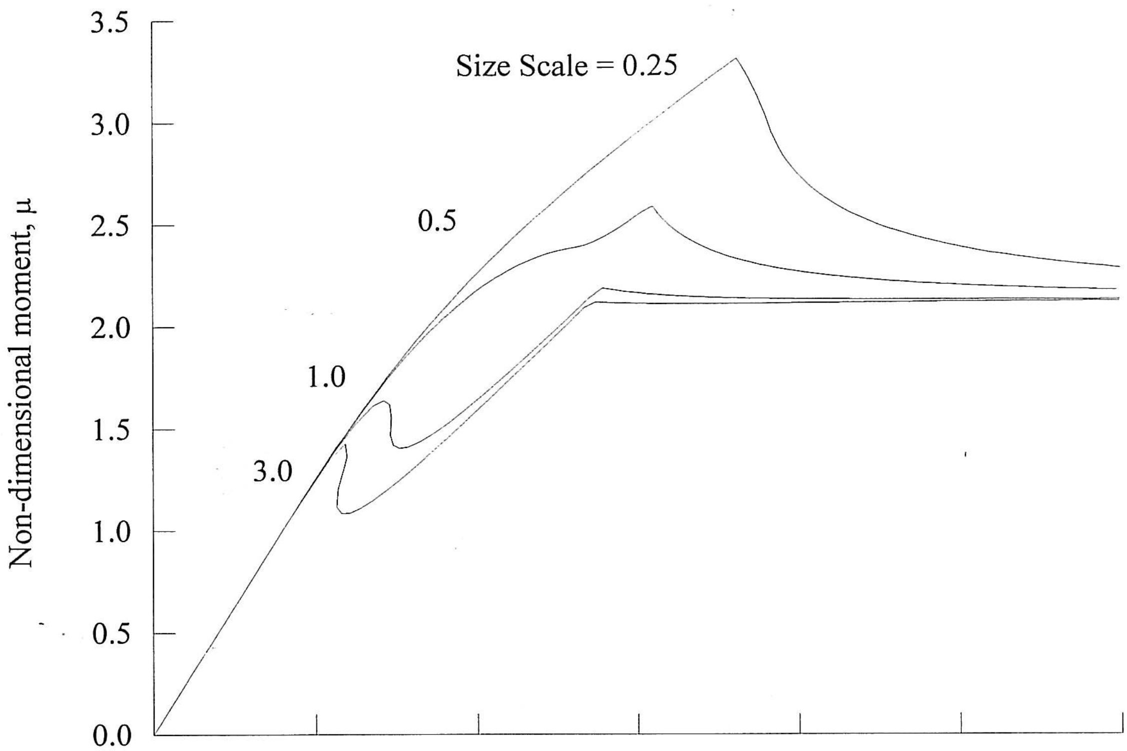


Fig. 4. Moment - rotation curves for beams at different size scales.

The shapes of the curves and the peak moment is seen to be dependent on both the reinforcement area and on the size of the structure. It is also seen that multiple cracking will occur for small size scales and large reinforcement areas.

## 5 Experiments

### 5.1 Materials

Concrete

A high strength concrete similar to the one used at the Great Belt project in Denmark has been used. The largest aggregate size in this concrete is, however, only 8 mm.

Table 2. Mix proportions, units are [kg/m$^3$].

| Cement | Fly ash | Silica fume | Water | Plas-tizice | Super Plast. | Sand | Gravel |
|---|---|---|---|---|---|---|---|
| 312 | 44 | 29 | 122 | 1.56 | 8.58 | 614 | 1238 |

Table 2. Mechanical properties of tested concrete, units are [MPa].

| Cylinder compres-sive strength | | Prism splitting strength | | Young's modulus | |
|---|---|---|---|---|---|
| Mean | S.Dev | Mean | S.Dev. | Mean | S.Dev. |
| 78,3 | 4.0% | 9.30 | 7.8% | 42660 | 2.5% |

Table 2. shows the mix of the concrete and Table 3. shows the mechanical properties.

Steel

Threaded steel bars were used as reinforcement instead on conventional reinforcement steel. This was done as conventional steel not was available in the small diameters that were used.Furthermore, this should reduce steel-concrete debonding. Un-notched and notched reinforcement were used. The notched reinforcement was used in the hope of eliminating debonding problems, and in this way being able to compare the test results to the model without taking debonding into account. Ordinary tension test were performed on 10 test bars. The test bars had a length of 360 mm and the nominal diameters were $d_{nom}$=3,4,5,6 and 8 mm. During testing it was observed that the steel did not show the normal yield tendency of soft steel and it had obviously been hardened under fabrication. Using linear regression the yield stress was found as $\sigma_y$= 588 MPa with a coefficient of variation of 3.5 % and the modulus of elasticity was $E_s$=1.83 $10^5$ MPa with a coefficient of variation of 1.6 %.

Specimen

The experiments were carried out on 2 different beam geometries (Size A: width and depth: 100 mm and span: 800 mm; Size B Width: 100 mm, depth: 200 mm; and span: 800 mm). These geometries were chosen for two reasons. Firstly, in order to be able to study structural size effects separately, and secondly because of the limitations of the testing equipment. A total amount of 38 beams were cast over a period of 4 weeks. The beams were named after size, batch number and reinforcement area (e.g. A-2-18.7 is beam size A made from batch number 2 and reinforced with 18.7 mm$^2$ steel ) . The day after casting the beams were striped from their molds and cured 11 days in hot water (37°C) and then 2 days in cold (20°C) . Then a notch of rectangular cross section was saw cut in the beams with a depth of 1/20 of the beam depth the day before testing.

### 5.2 Testing equipment and procedure

The beams were submitted to three-point bending in a servo-controlled materials testing system. In order to measure the true beam deflection a reference bar was placed on each side of the beam, and the beam deflection was measured as the distance from the load point to the reference bar using two LVDT's with a base of 20.0 mm and a sensitivity of 0.5 V/mm. The piston displacement was measured using the build-in LVDT with a base of 5.0 mm and a sensitivity of 2.0 V/mm. The crack opening displacement was measured using a clip-gauge with a base of 2.0 mm and with a sensitivity of 5.0 V/mm. The load was measured using a 50.0 kN load cell with a sensitivity of 0.2 V/kN. A schematic of the test set-up is shown in Fig. 3

All signals together with the time, $t$, were recorded using an analog to digital converter and an AT Personal Computer. The test was controlled by a feedback signal that included contributions from both the piston displacement and the COD. The feed back signal, $\delta$, was created by analog addition of the corresponding signals:

$$\delta=\alpha\delta_{COD}+\beta\delta_{p} \tag{15}$$

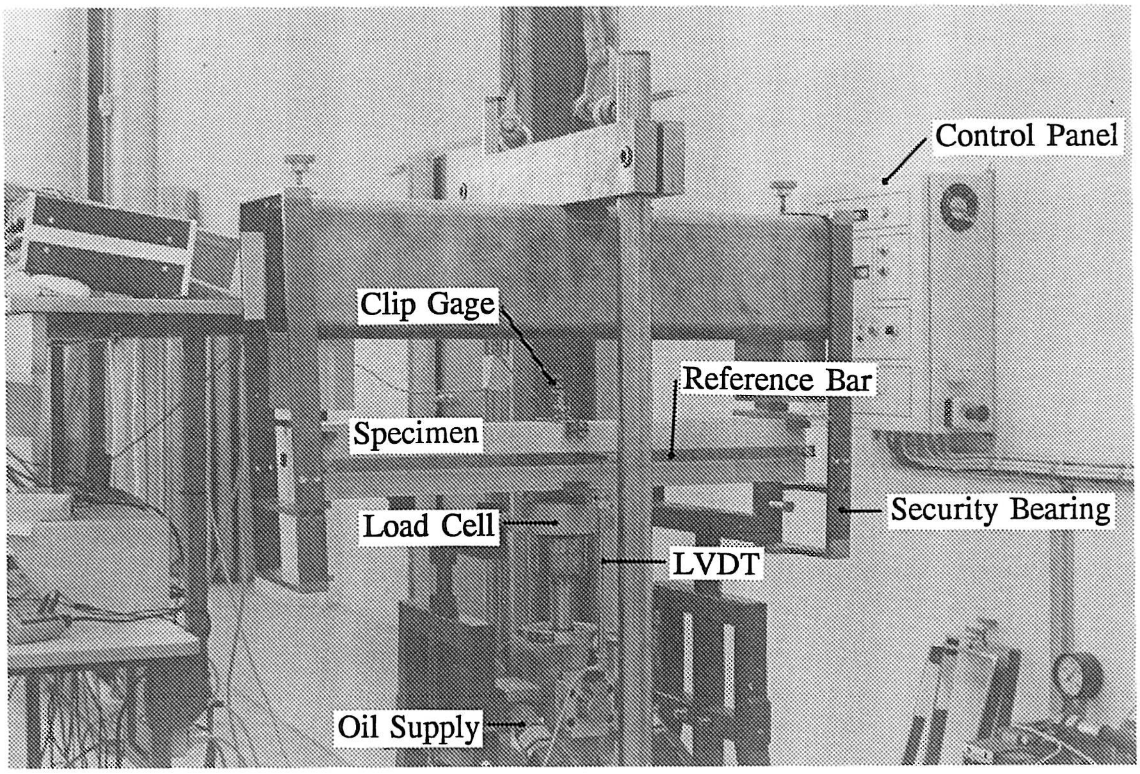


Fig. 5 Photo of test set-up.

where, $\delta_{COD}$, is the crack opening displacement and, $\delta_p$, is the piston displacement. The weight factors, $\alpha$, and, $\beta$, were chosen to $\alpha$=10.0 and 5.0 and $\beta$=1.0, where $\alpha$ is decreasing with the beam depth.

The reference signal, a linear ramp, was generated with the same AT PC using a digital to analog converter.

### 5.3 Fracture parameter results

8 plain concrete beams where tested in three point bending to determine the fracture parameters $\sigma_u$ and $G_F$.. The parameters where estimated using a numerical procedure called the direct sub-structure method, Brincker et al. (1989), Guessing the shape of the $\sigma$-w relation and using the Nelder and Mead scheme, Schittkowski (1985) an optimization was carried out to determine estimates the estimates of the two parameters. The method is fully described in Ulfkjær et al. (1992). The tensile strength was estimated to 7.39 MPa with a coefficient of variation of 6.4 % and the fracture energy was 0.131 $Nmm/mm^2$ with a coefficient of variation of 6.9 %.

## 6 Model Evaluation

Here comparison will only be made for notched steel. The material parameters described in the last section are used as input to the model. When calculating the dimensional moment the effective beam depth was used and when calculating the elastic deformations the total beam depth is used. In the following comparison is made between the model and the experimental results. The solid lines are the experiments and the dashed are the model curves. In Fig. 6-9 the results for series 4 are shown for beam size A with increasing reinforcement area. In Fig. 10-11 the results for series 7 for beam size B for two different reinforcement areas are shown. It is seen that the model predicts the stiffness of the beams very well, but the peak load is predicted too high for all reinforcement ratios and both sizes. This is due to the assumption of a linear softening relation which is not adequate. Instead a bi-linear softening relation should be used, Petersson (1981), Brincker and Dahl (1989). The intermediate phase of the fracture is not described to well, and it is assumed that this is due to the fact debonding is not taken into account. The yield load is described very well for most of the beams.

## 7 Conclusions

A simple analytical model for the response of reinforced beams in bending is developed by combining the fictitious crack model with linear elastic-perfectly plastic reinforcement action. The method gives explicit solutions for the moment-curvature relation and describes transitions from brittle to ductile behavior with changes in size scale and reinforcement ratio

Experiments where performed on high-strength concrete beams, and the fracture parameters where determined by using and indirect method. The results showed that the assumption of a linear softening relation is to crude and instead the equations should be

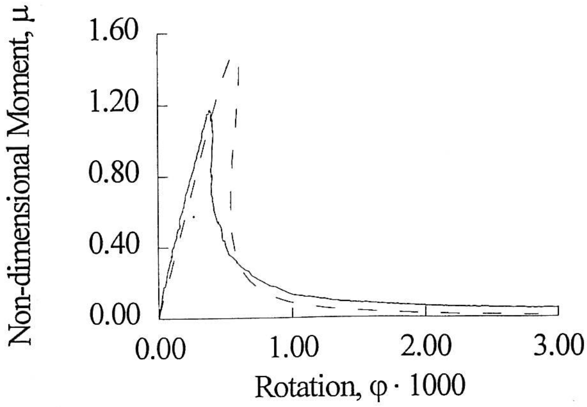


Fig. 6.Beam A-4-0.0 ($A_r$=0.0 $mm^2$)

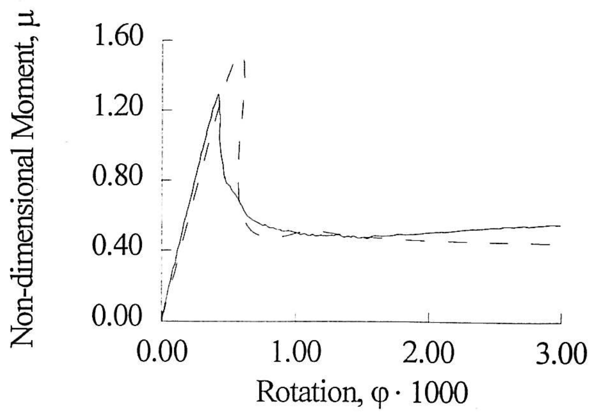


Fig. 7.Beam A-4-9.8 ($A_r$=9.8 $mm^2$)

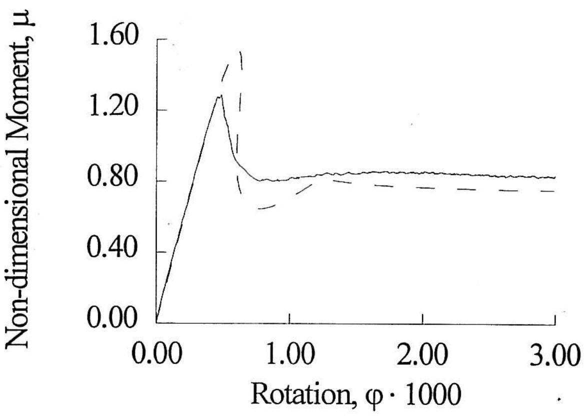


Fig. 8.Beam A-4-17.1 ($A_r$=17.1 $mm^2$)

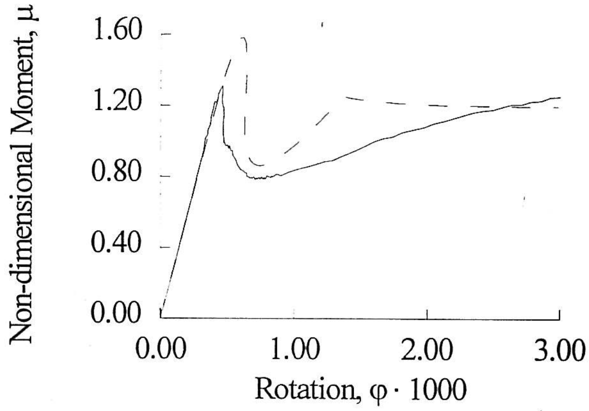


Fig. 9.Beam A-4-27.7 ($A_r$=27.7 $mm^2$)

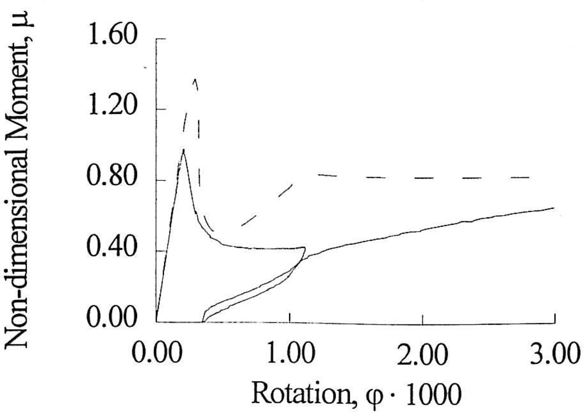


Fig. 10 Beam B-7-23.9 ($A_r$=23.9 $mm^2$).

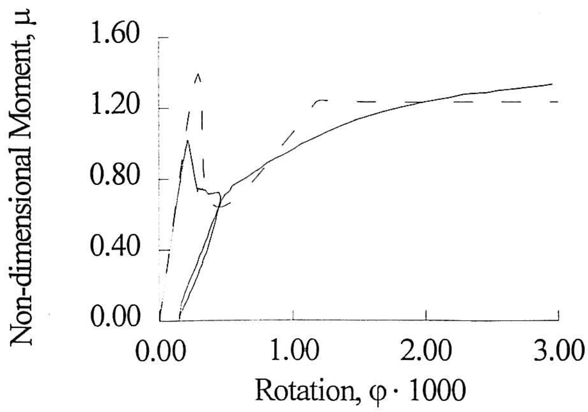


Fig. 11.Beam B-7-58.9 ($A_r$=58.9 $mm^2$)

derived for a bi-linear softening relation. It was also seen that the debonding problem should be taken into consideration.

## 8 References


Brincker, R. and Dahl, H. (1989), **Fictitious Crack Model of Concrete Fracture, Magazine of Concrete Research**, 41, No. 147, pp. 79-86.

Bosco, C. and Carpinteri, A. (1990), Fracture Mechanics Evaluation of Minimum Reinforcement in Concrete Structures, in **Application of Fracture Mechanics to Concrete Structures**, Edited by A. Carpinteri, Elsevier Applied Science, Italy, pp. 347-377.

Hededal, O. and Kroon, I.B. (1991), Lightly Reinforced High-Strength Concrete, **M.Sc Thesis at University of Aalborg**, pp. 1-88.

Modéer, M (1979), A Fracture Mechanics Approach to Failure Analysis of Concrete Materials, **Division of Building Materials, Lund Institute of Technology**, Ph.D.-thesis, Report TVBM-1001, Lund, Sweden, pp. 1-102.

Petersson, P-E. (1981), Crack Growth and Development of Fracture Zones in Plain Concrete and Similar Materials, **Division of Building Materials, Lund Institute of Technology**, TVBM-1006, Lund Sweden, pp.1-174.

Schittkowski, K. (1985), A FORTRAN subroutine Solving Constrained Non-Linear Programming Problems, **Annals of Operation Research**, Vol. 5, pp. 485-500.

Ulfkjær, J.P., Brincker, R. and Krenk, S. (1993), Analytical Model for Fictitious Crack Propagation in Concrete Beams, **Submitted for publication in Journal of Structural Engineering.**

Ulfkjær, J.P. and Brincker R. (1993), Indirect Determination of the σ-w relation of HSC Through Three-Point Bending, in **Fracture and Damage of Concrete and Rock, FDCR-2** (Edited by H.P. Rossmanith), Vienna, Austria, pp.135-144.

Van Mier, J.G.M. (1989), Other Applications, in **Fracture Mechanics of Concrete Structures- From Theory to Application** (Edited by L. Elfgren), Chapman and Hall, London, pp. 369-381.

## FRACTURE AND DYNAMICS PAPERS

PAPER NO. 21: P. H. Kirkegaard, J. D. Sørensen & Rune Brincker: *Optimization of Measurements on Dynamically Sensitive Structures Using a Reliability Approach.* ISSN 0902-7513 R9009.

PAPER NO. 22: Jakob Laigaard Jensen: *System Identification of Offshore Platforms.* ISSN 0902-7513 R9011.

PAPER NO. 23: Janus Lyngbye & Rune Brincker: *Crack Length Detection by Digital Image Processing.* ISSN 0902-7513 R9018.

PAPER NO 24: Jens Peder Ulfkjær, Rune Brinker & Steen Krenk: *Analytical Model for Complete Moment-Rotation Curves of Concrete Beams in bending.* ISSN 0902-7513 R9021.

PAPER NO 25: Leo Thesbjerg: *Active Vibration Control of Civil Engineering Structures under Earthquake Excitation.* ISSN 0902-7513 R9027.

PAPER NO. 26: Rune Brincker, Steen Krenk & Jakob Laigaard Jensen: *Estimation of correlation Functions by the Random Dec Technique.* ISSN 0902-7513 R9028.

PAPER NO. 27: Jakob Laigaard Jensen, Poul Henning Kirkegaard & Rune Brincker: *Model and Wave Load Identification by ARMA Calibration.* ISSN 0902-7513 R9035.

PAPER NO. 28: Rune Brincker, Steen Krenk & Jakob Laigaard Jensen: *Estimation of Correlation Functions by the Random Decrement Technique.* ISSN 0902-7513 R9041.

PAPER NO. 29: Poul Henning Kirkegaard, John D. Sørensen & Rune Brincker: *Optimal Design of Measurement Programs for the Parameter Identification of Dynamic Systems.* ISSN 0902-7513 R9103.

PAPER NO. 30: L. Gansted & N. B. Sørensen: *Introduction to Fatigue and Fracture Mechanics.* ISSN 0902-7513 R9104.

PAPER NO. 31: R. Brincker, A. Rytter & S. Krenk: *Non-Parametric Estimation of Correlation Functions.* ISSN 0902-7513 R9120.

PAPER NO. 32: R. Brincker, P. H. Kirkegaard & A. Rytter: *Identification of System Parameters by the Random Decrement Technique.* ISSN 0902-7513 R9121.

PAPER NO. 33: A. Rytter, R. Brincker & L. Pilegaard Hansen: *Detection of Fatigue Damage in a Steel Member.* ISSN 0902-7513 R9138.

PAPER NO. 34: J. P. Ulfkjær, S. Krenk & R. Brincker: *Analytical Model for Fictitious Crack Propagation in Concrete Beams.* ISSN 0902-7513 R9206.

PAPER NO. 35: J. Lyngbye: *Applications of Digital Image Analysis in Experimental Mechanics.* Ph.D.-Thesis. ISSN 0902-7513 R9227.

PAPER NO. 36: J. P. Ulfkjær & R. Brincker: *Indirect Determination of the $\sigma - w$ Relation of HSC Through Three-Point Bending.* ISSN 0902-7513 R9229.

## FRACTURE AND DYNAMICS PAPERS

PAPER NO. 37: A. Rytter, R. Brincker & P. H. Kirkegaard: *An Experimental Study of the Modal Parameters of a Damaged Cantilever.* ISSN 0902-7513 R9230.

PAPER NO. 38: P. H. Kirkegaard: *Cost Optimal System Identification Experiment Design.* ISSN 0902-7513 R9237.

PAPER NO. 39: P. H. Kirkegaard: *Optimal Selection of the Sampling Interval for Estimation of Modal Parameters by an ARMA-Model.* ISSN 0902-7513 R9238.

PAPER NO. 40: P. H. Kirkegaard & R. Brincker: *On the Optimal Location of Sensors for Parametric Identification of Linear Structural Systems.* ISSN 0902-7513 R9239.

PAPER NO. 41: P. H. Kirkegaard & A. Rytter: *Use of a Neural Network for Damage Detection and Location in a Steel Member.* ISSN 0902-7513 R9245

PAPER NO. 42: L. Gansted: *Analysis and Description of High-Cycle Stochastic Fatigue in Steel.* Ph.D.-Thesis. ISSN 0902-7513 R9135.

PAPER NO. 43: M. Krawczuk: *A New Finite Element for Static and Dynamic Analysis of Cracked Composite Beams.* ISSN 0902-7513 R9305.

PAPER NO. 44: A. Rytter: *Vibrational Based Inspection of Civil Engineering Structures.* Ph.D.-Thesis. ISSN 0902-7513 R9314.

PAPER NO. 45: P. H. Kirkegaard & A. Rytter: *An Experimental Study of the Modal Parameters of a Damaged Steel Mast.* ISSN 0902-7513 R9320.

PAPER NO. 46: P. H. Kirkegaard & A. Rytter: *An Experimental Study of a Steel Lattice Mast under Natural Excitation.* ISSN 0902-7513 R9326.

PAPER NO. 47: P. H. Kirkegaard & A. Rytter: *Use of Neural Networks for Damage Assessment in a Steel Mast.* ISSN 0902-7513 R9340.

PAPER NO. 48: R. Brincker, M. Demosthenous & G. C. Manos: *Estimation of the Coefficient of Restitution of Rocking Systems by the Random Decrement Technique.* ISSN 0902-7513 R9341.

PAPER NO. 49: L. Gansted: *Fatigue of Steel: Constant-Amplitude Load on CCT-Specimens.* ISSN 0902-7513 R9344.

PAPER NO. 50: P. H. Kirkegaard & A. Rytter: *Vibration Based Damage Assessment of a Cantilever using a Neural Network.* ISSN 0902-7513 R9345.

PAPER NO. 51: J. P. Ulfkjær, O. Hededal, I. B. Kroon, R. Brincker: *Simple Application of Fictitious Crack Model in Reinforced Concrete Beams.* ISSN 0902-7513 R9349.

PAPER NO 52: J. P. Ulfkjær, O. Hededal, I. B. Kroon, R. Brincker: *Simple Application of Fictitious Crack Model in Reinforced Concrete Beams. Analysis and Experiments.* ISSN 0902-7513 R9350.

**Department of Building Technology and Structural Engineering**
**The University of Aalborg, Sohngaardsholmsvej 57, DK 9000 Aalborg**
**Telephone: 45 98 15 85 22 Telefax: 45 98 14 82 43**